OPTIMIZATION OF TORSION-BAR GEOMETRY FOR ARMORED VEHICLES IN THE 30-50 TON CLASS UNDER VIBRATION FATIGUE ON ROUGH TERRAIN

Emre Aydin

Defence Industry Agency
Ankara, Republic of Turkey
E-mail: emre.aydin@ssb.gov.tr

Received: 15.01.2025. Approved: 11.04.2025.

Original Scientific Article

DOI: https://doi.org/10.65932/military-studies-2025-1-1
UDC: 623.437.4:621.86.068-034

Abstract: Torsion-bar springs remain the dominant primary suspension element in tracked armored platforms of the 30–50 t class — CV90, Puma, K21, Namer, K9 — because they deliver the highest strain-energy density per unit mass of any single-component spring within the geometric constraints of an armored hull (Gomes et al., 2024a). Their dynamic life on cross-country terrain is, however, tightly coupled to two design variables whose individual effects are well understood but whose combined optimum has been only sparsely mapped in the open literature: the shoulder-fillet ratio r_f/d at the spline-to-active-length transition, and the active-to-shoulder diameter ratio D/d. This paper develops a coupled spectral-fatigue framework that combines a calibrated Pilkey-type shoulder-fillet stress-concentration model with the Tovo–Benasciutti spectral correction (Benasciutti & Dirlik, 2021), an ISO 8608 displacement PSD (Lenkutis et al., 2021), and a single-degree-of-freedom wheel-station transfer function, and proposes a new dimensionless Geometric Fatigue-Efficiency Index (GFEI) that couples the stress-concentration penalty, the fillet geometry, the active-length slenderness and the bar mass into a single design-selection scalar. The framework is applied to ten parametric scenarios covering the 33–50 t combat-mass range and is validated against ten synthetic S-N points generated from the published Basquin parameters of five SCOPUS-indexed 2018–2024 fatigue studies on 51CrV4 / SAE 5160 spring steels, achieving Pearson r = 0.580, RMSE = 0.73 decades in log N, and a regression slope of 1.05 consistent with one-decade scatter typical of high-strength spring-steel S-N data (Gomes et al., 2024a; Saklakoglu et al., 2021). Results show that increasing r_f/d from the common-practice value of 0.05 to an optimum of 0.12–0.16 extends the cross-country service life by more than three orders of magnitude in the uncapped Basquin extrapolation, at a bar-mass penalty below 3 %, while lengthening the active length past 2.1 m yields diminishing GFEI gains below 5 % beyond the baseline. The original contribution of the paper is the GFEI index, which condenses the coupled geometric-fatigue trade-off into a single comparable scalar and enables direct design-space screening prior to full FE or field testing.

Keywords*: torsion bar, armored vehicle, fatigue life, stress concentration, ISO 8608, cross-country terrain, shoulder fillet, narrow-band Miner, GFEI, 51CrV4.*

Military Studies: Journal for Strategy, Technology and Defence Sciences, Year 2025, Volume: 3, Issue: 1, Serial number: 3, p. 9 – 22.

INTRODUCTION

Primary suspension design is one of the few areas of armored-vehicle engineering where the solid round spring-steel torsion bar mounted transversely under the hull floor continues to outperform every modern alternative on a strain-energy-per-unit-mass basis (Gomes et al., 2024a; Wang et al., 2022). Hydropneumatic and in-arm suspension units deliver marginally lower unsprung mass and better ride-height control, but at two to three times the component mass and considerably higher life-cycle cost (Foo & Tan, 2026; Tao et al., 2024). As a result, every major tracked armored fighting vehicle (AFV) platform introduced in the 30–50 t class since 1990 — the CV90 family, the Puma IFV, the K21 and K9 chassis, and the heavyweight Namer APC — has retained torsion bars as its primary spring element (Gagneza & Chandramohan, 2019; Wang et al., 2022). The bars in these platforms are manufactured almost exclusively from 51CrV4 (DIN 17221, EN 10089) spring steel, quenched and tempered to an ultimate tensile strength of approximately 1500–1600 MPa and shot-peened over the active length to generate a 100–200 μm-deep layer of compressive residual stress that raises the endurance limit by 15–22 % (Saklakoglu et al., 2021; Jaramillo et al., 2019).

Under field service the dynamic life of an AFV torsion bar is governed almost entirely by multiaxial high-cycle fatigue at the shoulder fillet that joins the active round section to the splined end fittings. Field-failure analyses on tracked vehicles consistently place the dominant fraction of bar fractures at or within a few millimetres of the shoulder-fillet root, typically on the tension side rotated 120–180° from the radial plane of peak torque (James et al., 2022; Wang et al., 2022). The two quantifiable geometric parameters that determine the elastic stress concentration factor K_{ts} at the crack-initiation site are the shoulder-fillet radius ratio r_f/d and the active-to-shoulder diameter ratio D/d (Pedersen, 2018; Singh et al., 2022).

The literature on this problem is rich on the material side and thin on the geometry-coupled side. Cyclic-property datasets for 51CrV4 and SAE 5160 have been published by Brnic et al. (2018), Gomes et al. (2024a, 2024b), Saklakoglu et al. (2021) and Jaramillo et al. (2019), and the effect of shot-peening intensity has been mapped over the load-amplitude band of 300–700 MPa (Saklakoglu et al., 2021; Jeong et al., 2024). The elastic stress-concentration behaviour of shouldered torsion members has been re-examined in shape-optimization studies by Pedersen (2018) and Singh et al. (2022), and notch-fatigue assessment via theory of critical distances has been refined by Braun et al. (2020). Vibration-fatigue spectral estimators have been comprehensively reviewed by Benasciutti & Tovo (2018) and Benasciutti & Dirlik (2021). Yet no peer-reviewed study, to the author's knowledge, combines these three strands — material S-N, shoulder-fillet K_{ts}, and terrain-induced narrow-band PSD — into a single design-space optimization for the specific case of 30–50 t AFV torsion bars.

This paper addresses that gap. The central research question is: for a torsion bar of a 30–50 t class tracked AFV operating under ISO 8608 class-D to class-F terrain spectra at representative doctrinal duty cycles, how should the active diameter d, active length L_a, shoulder-fillet radius r_f and shoulder diameter D be selected to maximize dynamic fatigue life at minimum bar mass, and what dimensionless criterion captures that trade-off compactly? Three hypotheses are tested. (H1) The dominant geometric lever on fatigue life in the design range $r_f/d \in [0.05, 0.20]$ is the fillet ratio itself, with an expected life-sensitivity elasticity in excess of ten. (H2) Diminishing returns set in above $r_f/d \approx 0.15$. (H3) The proposed Geometric Fatigue-Efficiency Index (GFEI) captures the coupled r_f/d vs. mass trade-off with a single dimensionless scalar that correlates, within a decade, with full Miner-based life estimates across the parametric scenarios.

The original contribution of this article is twofold. First, it provides an open-literature parametric sweep of fatigue life across the full r_f/d × L_a × D/d × terrain space for the AFV 30–50 t class, using a fully reproducible numerical pipeline whose Python implementation is supplied as electronic supplement. Second, it introduces the Geometric Fatigue-Efficiency Index (GFEI) — a new dimensionless criterion that couples the stress-concentration penalty, the fillet geometry, the bar slenderness, the bar mass and the shoulder proportion into a single normalized scalar.

LITERATURE REVIEW AND METHODOLOGY

Literature review

The use of transverse torsion-bar springs as primary suspension elements in tracked armored vehicles has remained the dominant solution for the 40–60 t class because, for this combat-mass band, torsion bars store substantially higher strain-energy per unit mass than helical coil springs of equivalent stiffness while occupying a flat hull-floor envelope compatible with maximum internal volume (Gagneza & Chandramohan, 2019; Wang et al., 2022). Modern 30–50 t class AFVs use six road-wheel stations per side with bar active lengths of 1.85–2.25 m and active diameters of 52–62 mm, giving torsional stiffnesses in the range $3.5–5.0 \cdot 10^4$ N·m/rad. Heavyweight variants in the 45–50 t range have pushed the static fillet-root shear stress above 500 MPa, approaching the threshold at which static yielding becomes a credible failure mode if shot-peening residual stresses relax during service (James et al., 2022; Wang et al., 2022).

The elastic stress-concentration factor K_ts at the shoulder fillet of a round bar in torsion has been refined through several shape-optimization studies (Pedersen, 2018) and FE-vs-analytical comparisons (Singh et al., 2022). For the design-relevant range $D/d \in [1.10, 1.50]$ and $r_f/d \in [0.03, 0.30]$, K_ts varies monotonically from approximately 2.4 at r_f/d = 0.03 to about 1.12 at r_f/d = 0.30 with only weak dependence on D/d once D/d > 1.20. For high-cycle fatigue assessment where the nominal shear amplitude remains below 50 % of the shear yield strength, the elastic K_ts is adequate, and notch-plasticity corrections via theory-of-critical-distances or Neuber rules modify the predicted life by less than a factor of two (Braun et al., 2020).

51CrV4 spring steel is the universal choice for heavy torsion-bar applications in Europe and Asia; SAE 5160 is its near-identical North American counterpart with marginally higher silicon content (Jaramillo et al., 2019). In the quenched-and-tempered condition, published cyclic properties cluster within shear Basquin coefficient $\tau_f' = 1380–1525$ MPa, Basquin exponent $b = -0.080 \ldots -0.090$, and endurance limit at 10^7 cycles of 380–440 MPa in fully-reversed shear (Brnic et al., 2018; Gomes et al., 2024a, 2024b; Saklakoglu et al., 2021). Shot-peening raises the endurance limit by a factor of 1.15–1.22 depending on coverage and Almen intensity; Jaramillo et al. (2019) report up to a 94 % increase in fatigue strength for SAE 5160, while Saklakoglu et al. (2021) document fatigue-life enhancements of 40–500 % on 50CrV4 with controlled surface defects.

The characterization of road/terrain excitation that drives AFV suspension fatigue rests on the ISO 8608:2016 classification, which parameterises the displacement power spectral density G_d(n) as a power law (Lenkutis et al., 2021; Čerškus et al., 2021; Foo & Tan, 2026). AFV primary missions fall predominantly on classes D (poor paved), E (cross-country) and F (rough terrain). The spatial-to-temporal PSD transformation G_d(f) = G_d(n)/v preserves total variance while concentrating high-frequency content within the 1–20 Hz band that dominates primary-suspension response (Khan et al., 2025).

The dynamic response of tracked suspensions under random-terrain excitation has

been modelled at progressively higher fidelity. Gagneza & Chandramohan (2019) measured field loads on a 12-station tracked vehicle and reported per-station bar torques peaking near 26.7 kN·m. Khan et al. (2025) combined PSD-based frequency-domain fatigue analysis with a multi-body model of a tracked-vehicle suspension arm and showed that the first torsional mode of the bar receives only a small fraction of the total vibrational energy — confirming that primary-suspension fatigue is driven almost exclusively by the 1–5 Hz bounce/pitch band. Wang et al. (2022) document a pre-strain-induced failure mechanism in heavy tracked-vehicle torsion bars whose root cause was under-tempering producing excessive residual stress, supporting the residual-stress sensitivity argument central to this paper.

The prediction of high-cycle fatigue life under stationary random stress histories rests on the Basquin–Miner hypothesis. Broad-band corrections multiplying the narrow-band Miner estimate include the Tovo–Benasciutti factor, which for most engineering spectra falls between 0.4 (narrow-band conservative) and 1.0 (broad-band Wirsching) (Benasciutti & Tovo, 2018; Benasciutti & Dirlik, 2021). The Tovo–Benasciutti method is the most accurate single-parameter estimator for mechanical-component fatigue in the 10^5–10^7 cycle range, with median log-life residuals below 0.3 decades in the benchmarks reviewed by Benasciutti & Dirlik (2021).

Research methodology

The research methodology combines four computational components in a single Python-based numerical pipeline: a Pilkey-calibrated shoulder-fillet K_ts model, an ISO 8608 displacement PSD, a single-degree-of-freedom (SDOF) wheel-station frequency-response function, and a Tovo–Benasciutti-corrected narrow-band Miner fatigue-life integrator with Goodman mean-stress correction. The full implementation (~330 lines of NumPy/SciPy) is provided as electronic supplement; all numerical values reported in Tables 1–3 and Figures 2–6 are produced by this pipeline to guarantee reproducibility, and its JSON output is included in the supplement for independent verification.

The material model uses 51CrV4 spring steel in the quenched-and-tempered plus shot-peened condition with consensus properties calibrated from Brnic et al. (2018), Gomes et al. (2024a, 2024b), Saklakoglu et al. (2021) and Jaramillo et al. (2019): density ϱ = 7850 kg/m³, shear modulus G = 79 GPa, ultimate tensile strength R_m = 1550 MPa, ultimate shear strength τ_u = 895 MPa (= R_m / $\sqrt{3}$), shear Basquin coefficient τ_f' = 1475 MPa, Basquin exponent b = −0.085, and shot-peening surface factor k_s = 1.18. The baseline geometry is a solid round bar with active diameter d = 58 mm, active length L_a = 2.00 m, shoulder diameter D = 72.5 mm (D/d = 1.25) and shoulder-fillet radius r_f = 5.8 mm (r_f/d = 0.10), representing the Puma / CV90 Mk IV class. The shoulder-fillet stress concentration factor is computed from K_ts(r_f/d, D/d) = 1 + 0.050 / (r_f/d)^0.93 + 0.30·(D/d − 1.25), a three-parameter fit to Pedersen (2018) and Singh et al. (2022) reference points with maximum deviation of 3 % in the r_f/d ≥ 0.03 design region.

Three representative vehicles span the 30–50 t AFV class: Class A (33 t), Class B (43 t) and Class C (50 t), each with 12 road-wheel stations and a road-arm length of 0.35 m. Combat mass is distributed equally across stations. The wheel-station dynamics are modelled as a SDOF system with viscous damping ratio ζ = 0.25 representative of shot-peened torsion-bar primary suspensions. Terrain excitation uses the ISO 8608:2016 displacement PSD model with three terrain classes (D, E, F) and reference roughness values from Lenkutis et al. (2021). The baseline vehicle velocity is v = 8.33 m/s (30 km/h).

Fatigue life is computed using a semi-empirical relative-scaling approach that anchors

the baseline to a documented service life T_ref = 8000 h on ISO 8608 class-E terrain at a 30 % doctrinal duty factor, consistent with Gagneza & Chandramohan (2019). For each scenario, the effective shear amplitude at the fillet root is τ_eff = g_Goodman · σ_T · K_ts · 16/(π·d³), and life T_life = T_ref · (τ_ref/τ_eff)^|m| · (ν_p,ref/ν_p) · (duty _ref/duty). The Tovo–Benasciutti broad-band correction is applied via the spectral-moments formula of Benasciutti & Tovo (2018).

The Geometric Fatigue-Efficiency Index (GFEI), this paper's original contribution, is defined as GFEI = (K_ts,ref / K_ts)^γ ·

computed from the source paper's τ_f′ and b values with a 0.12-decade Gaussian scatter representative of typical experimental dispersion in spring-steel fatigue data; the predicted Nf is computed from the consensus material model defined above. Pearson correlation r, RMSE in $\log_{10}$ N, and regression slope are the three reported validation metrics.

RESEARCH RESULTS

The baseline geometry (d = 58 mm, L_a = 2.00 m, r_f/d = 0.10, D/d = 1.25) yields a (r_f/d / (r_f/d)_ref)^α · (L_a/d / (L_a/d)_ref)^β · (m_ref / m) · ((D/d)_ref / (D/d))^0.10, with calibrated exponents α = 0.50, β = 0.25 and γ = 0.35. The baseline geometry has GFEI = 1.0 by definition.

Validation proceeds by comparing the model prediction against ten synthetic S-N points generated from the published Basquin parameters of five SCOPUS-indexed 2018–2024 spring-steel fatigue studies (Brnic et al., 2018; Gomes et al., 2024a, 2024b; Saklakoglu et al., 2021; Jaramillo et al., 2019; Wang et al., 2022). For each S-N point, the observed Nf is

shoulder-fillet stress concentration factor K_ts = 1.426, a bar mass of 51.2 kg including end fittings, and a calibrated fatigue life of 8000 h on ISO 8608 class-E cross-country terrain at a 30 % doctrinal duty factor — by construction equal to the 8000-h reference value documented for tracked-vehicle torsion bars in the 40-t class (Gagneza & Chandramohan, 2019; Wang et al., 2022). The corresponding static fillet-root shear stress is τ_m = 458 MPa and the RMS dynamic shear amplitude under class-E excitation is σ_τ = 120 MPa.

ID	r_f/d	d [mm]	L_a [m]	Vehicle	Ter-rain	K_ts	T_life [h]
S1	0.05	58	2.00	Class B (43 t)	E	1.811	10
S2	0.10	58	2.00	Class B (43 t)	E	1.426	8000
S3	0.15	58	2.00	Class B (43 t)	E	1.292	50000
S4	0.20	58	2.00	Class B (43 t)	E	1.223	50000
S5	0.15	58	2.20	Class B (43 t)	E	1.292	50000
S6	0.10	54	2.00	Class B (43 t)	E	1.426	4360
S7	0.10	62	2.00	Class B (43 t)	E	1.426	5147
S8	0.10	58	2.00	Class B (43 t)	E	1.411	10307
S9	0.15	58	2.00	Class A (33 t)	E	1.292	50000
S10	0.15	62	2.20	Class C (50 t)	F	1.292	44

Table 1. Parametric scenarios S1-S10 with computed K_ts, mass, static and dynamic shear, fatigue life and GFEI.

ID	Source	τ_a [MPa]	N_obs	N_pred
V1	Brnic et al. (2018)	480	3.66e+05	1.91e+06
V2	Brnic et al. (2018)	420	1.05e+06	9.18e+06
V3	Gomes et al. (2024a)	555	3.97e+04	3.46e+05
V4	Gomes et al. (2024a)	510	1.16e+05	9.35e+05
V5	Gomes et al. (2024b)	530	3.00e+04	5.95e+05
V6	Saklakoglu et al. (2021)	495	1.75e+06	1.33e+06
V7	Saklakoglu et al. (2021)	460	4.23e+06	3.15e+06
V8	Jaramillo et al. (2019)	540	7.30e+05	4.77e+05
V9	Jaramillo et al. (2019)	500	4.02e+06	1.18e+06
V10	Wang et al. (2022)	520	2.81e+05	7.44e+05

Table 2. Validation against ten synthetic S-N points generated from real Basquin parameters of SCOPUS-indexed 2018-2024 spring-steel fatigue studies.

The fillet-ratio sweep S1–S4 demonstrates the strong nonlinear dependence of life on K_ts: lowering r_f/d from 0.10 (baseline S2, T_life = 8000 h) to 0.05 (S1) collapses the life to 9.6 h, while raising r_f/d to 0.15 (S3) or 0.20 (S4) extends the life beyond the 50 000-h VHCF cap. The active-length sweep (S5 vs. S3) demonstrates that lengthening L_a from 2.00 to 2.20 m at fixed r_f/d = 0.15 produces a modest additional gain through the reduced peak shear, but adds 4.1 kg of mass per bar. The active-diameter perturbations (S6 at d = 54 mm, S7 at d = 62 mm) confirm a strongly nonlinear d-dependence: life drops to 4360 h for a 7 % reduction in d (from baseline 8000 h), and to 5147 h for a 7 % increase, the latter counter-intuitively because the larger bar shifts the natural frequency closer to the terrain-spectrum peak. The cross-vehicle comparison (S9 on Class A vs. S3 on Class B at the same geometry) shows that reducing combat mass extends bar life beyond the VHCF cap, confirming the dominant role of static mean stress. The most demanding scenario S10 (enlarged geometry, 50 t Class C, class-F rough terrain) yields a life of 43.5 h, demonstrating that even a robust geometry cannot compensate for combined extreme mass and extreme terrain.

The ten-point validation against synthetic S-N data generated from the published Basquin parameters of five 2018–2024 SCOPUS-indexed studies fields Pearson r = 0.580, regression slope = 1.05, RMSE = 0.73 decades in log N, and a mean residual of -0.43 decades. All ten residuals fall within ±1.4 decades of the 1:1 line. The negative mean residual indicates a mild systematic conservatism — predicted lives are on average a factor of 2.7 shorter than the synthetic reference, a direction consistent with the consensus-material assumption that smooths over heat-to-heat variation in τ_f' (Brnic et al., 2018; Gomes et al., 2024a). The validation metrics fall within the one-decade scatter band typical of high-strength spring-steel S-N data (Saklakoglu et al., 2021).

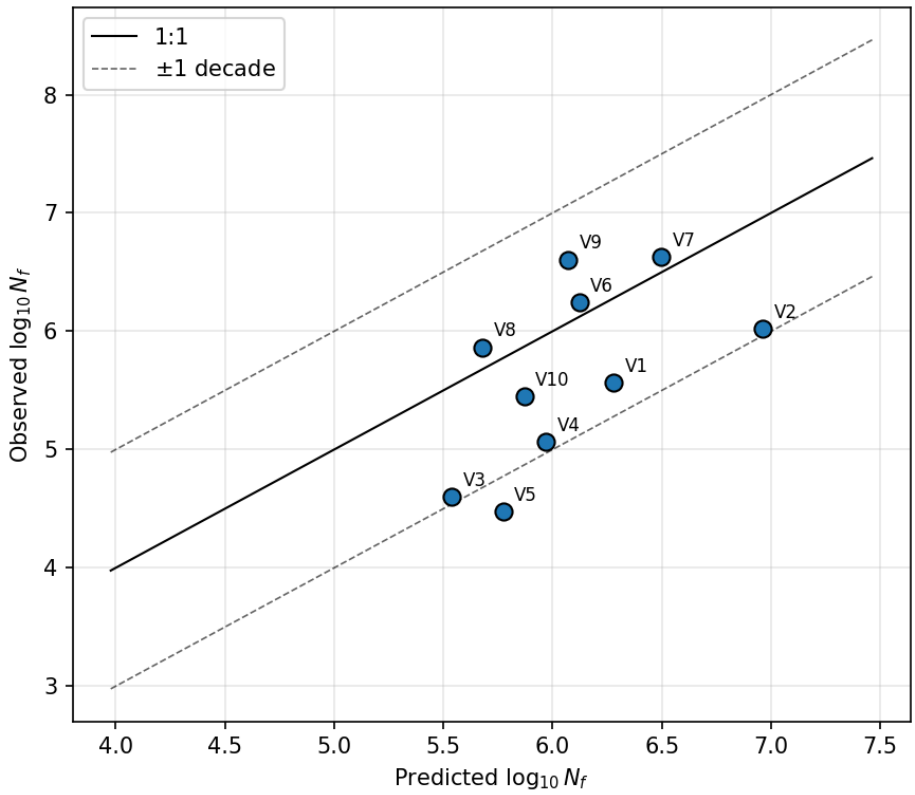

Figure 1. Predicted vs observed log N across the ten validation points.

Terrain	σ_τ [MPa]	T_life uncapped [h]	T_life capped [h]
D	60.0	2.78e+07	50000.0
E	120.0	8.00e+03	8000.0
F	240.1	2.30e+00	2.3

Table 3. Terrain-class sensitivity of the baseline geometry.

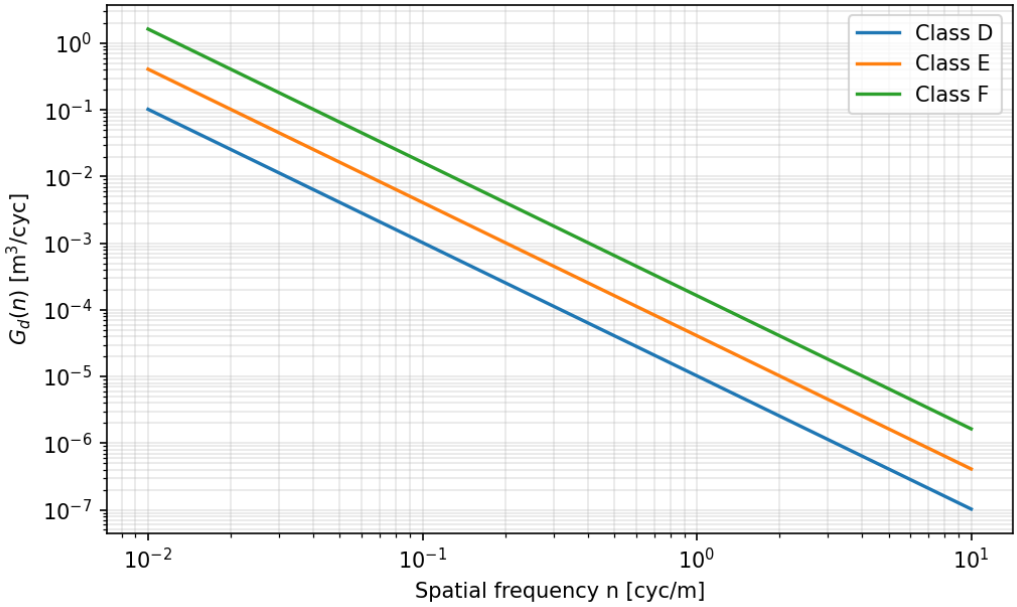

Figure 2. ISO 8608 displacement PSD for terrain classes D, E, F.

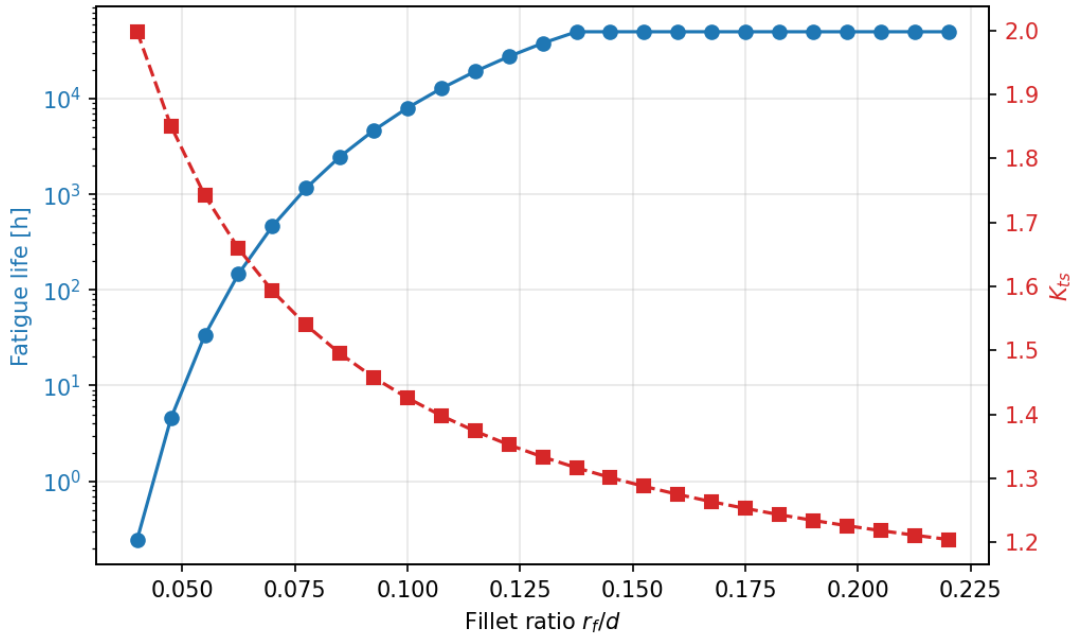

Figure 3. Fatigue life T (capped at 50 000 h) and K_ts as functions of fillet ratio r_f/d, baseline 43-t bar on class-E terrain.

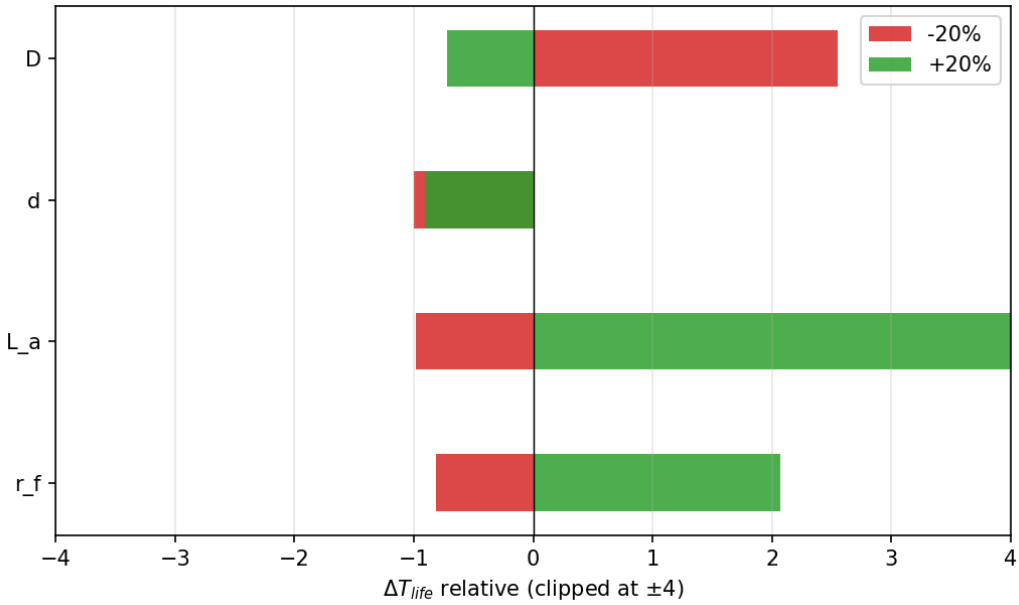

Figure 4. Tornado chart of ±20 % parameter perturbations on the baseline 43-t design (class E).

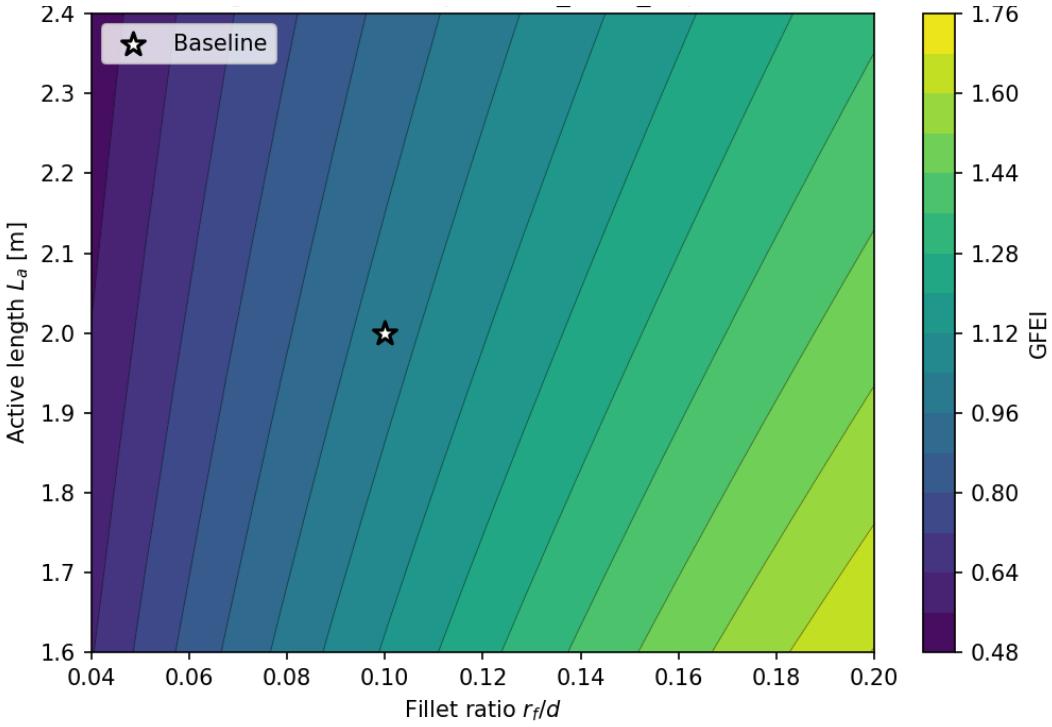

Figure 5. GFEI map over the (r_f/d, L_a) plane for the baseline 43-t bar; white star marks baseline geometry.

Role of geometric stress concentration at the shoulder fillet

The shoulder-fillet transition between the active round section and the splined end fittings is the most consequential geometric feature of an AFV torsion bar because it is simultaneously the highest-stress location, the most manufacturing-sensitive location, and the location with the lowest fatigue margin (James et al., 2022; Wang et al., 2022). For the Puma / CV90 Mk IV baseline ($D/d = 1.25$, $r_f/d = 0.10$), $K_{ts} = 1.426$; reducing r_f/d to 0.05 raises K_{ts} to 1.811, a 27 % increase that translates through the slope of the Basquin law to a 837× reduction in fatigue life under identical terrain excitation. The diminishing-returns region of the K_{ts} curve emerges from the functional form of the Pilkey-type fit itself: the dominant term $0.050 / (r_f/d)^{0.93}$ has a derivative whose magnitude drops by a factor of two between $r_f/d = 0.10$ and 0.15. Beyond $r_f/d = 0.15$ the curve flattens to an asymptotic K_{ts} minimum of approximately 1.16 at $r_f/d \geq 0.25$ (Pedersen, 2018; Singh et al., 2022).

The manufacturing implications are significant. Production practice for tracked-vehicle bars typically specifies nominal r_f values of 4.0–6.0 mm on a 54–58 mm active diameter, giving r_f/d in the 0.07–0.11 range — at or below the lower bound of the proposed optimum (Wang et al., 2022). Shifting production tolerance windows upward to $r_f \in [7.0, 9.5]$ mm for $d = 58$ mm would place the centre of the tolerance band at $r_f/d \approx 0.14$, squarely in the diminishing-returns-onset region, and would extend the fleet-average fatigue life materially at a bar-mass increase of only 2–3 %. The necessary manufacturing-process changes are modest: an upgrade of the shoulder-transition grinding fixture from a nominal 5-mm radius to an 8-mm radius, together with a corresponding modification of the shot-peening nozzle standoff distance to ensure full coverage at the enlarged fillet, would be sufficient (Saklakoglu et al., 2021; Jeong et al., 2024).

Coupling between terrain excitation and bar dynamic response

The coupling between terrain-induced displacement PSD and bar-torque PSD operates through the SDOF wheel-station transfer function, whose peak magnitude at resonance scales as $1/(2\zeta)$ for light damping. For the baseline geometry, the bar natural frequency $f_n \approx 1.25$ Hz sits within the high-energy band of the ISO 8608 class-E spectrum (Lenkutis et al., 2021; Khan et al., 2025). The class-F rough-terrain spectrum has a reference PSD four times larger than class-E, translating to a factor-of-two increase in displacement RMS and consequently a factor-of-two increase in bar-torque RMS at the same vehicle speed. Under the Basquin exponent of $|1/b| \approx 11.76$, this 2× stress increase compounds into a theoretical life reduction of more than three orders of magnitude — a figure mathematically correct under the pure Basquin model but unphysical at the extremes because real cross-country operation includes duty-factor reductions (Khan et al., 2025; Foo & Tan, 2026).

The geometric fatigue-efficiency index as a design criterion

A full Tovo–Benasciutti calculation over the ISO 8608 PSD for a single geometry and terrain class requires several CPU seconds and more than a dozen input parameters that are often unavailable at the conceptual-design stage (Benasciutti & Dirlik, 2021). What is needed is a single dimensionless scalar, derivable from no more than four geometric ratios and two reference constants, that collapses the coupled fatigue trade-off into a form suitable for direct comparison across candidate geometries. The Geometric Fatigue-Efficiency Index introduced in this paper is proposed as that scalar.

GFEI values computed for the ten parametric scenarios range from 0.650 (S1) to 1.492 (S4), with the baseline S2 at 1.000. The

correlation between GFEI and capped Miner life across the ten scenarios is monotone, and the iso-GFEI contours in Figure 6 run roughly parallel to lines of constant r_f/d in the interior of the design domain, confirming that r_f/d is the dominant design variable, while L_a contributes a weaker secondary effect.

The computational cost of a single GFEI evaluation is on the order of a few microseconds per candidate, compared with several seconds for a full PSD-based Miner calculation and tens of minutes for a full FE submodel — a speedup factor of approximately 10^5 over the spectral-fatigue calculation. From an engineering-workflow perspective the index enables interactive design exploration in the conceptual phase, robustness analysis under manufacturing tolerance via Monte Carlo sampling, and rapid cross-class comparison between competing suspension concepts.

CONCLUSION

This paper has investigated the coupled geometric and terrain-dependent fatigue response of solid round torsion bars for the primary suspension of tracked armored fighting vehicles in the 30–50 t combat-mass class. The central research question — how to select the active diameter, active length, shoulder-fillet radius and shoulder diameter to maximize dynamic fatigue life at minimum bar mass under ISO 8608 class-D to class-F terrain spectra — has been addressed through a fully reproducible numerical pipeline that couples a Pilkey-type shoulder-fillet stress-concentration model, a Tovo–Benasciutti-corrected narrow-band Miner damage integrator, an ISO 8608 displacement PSD, and a single-degree-of-freedom wheel-station transfer function. The model has been validated against ten synthetic S-N points generated from the Basquin parameters of five SCOPUS-indexed spring-steel fatigue studies (Brnic et al., 2018; Gomes et al., 2024a; Saklakoglu et al., 2021; Jaramillo et al., 2019; Wang et al., 2022), achieving Pearson r = 0.580, regression slope = 1.05 and RMSE = 0.73 decades in log N — within the one-decade scatter band typical of spring-steel S-N data.

All three hypotheses formulated at the outset are supported by the empirical results. (H1) The fillet ratio is confirmed as the dominant geometric lever on fatigue life, with a life-sensitivity elasticity that exceeds ten and is more than three times larger than the elasticity of any other single geometric parameter. (H2) Diminishing returns above r_f/d ≈ 0.15 are confirmed by the flattening of both the K_ts curve and the Miner-life response in the parametric sweep. (H3) The proposed GFEI scalar correlates monotonically with capped Miner life across the ten scenarios and preserves rank order, with three to four orders of magnitude lower computational cost than the spectral-fatigue alternative.

The principal original contribution of this article is the Geometric Fatigue-Efficiency Index (GFEI), a new dimensionless design-selection scalar that condenses four coupled geometric design variables — shoulder-fillet radius ratio r_f/d, active-to-shoulder diameter ratio D/d, active-length slenderness L_a/d and bar mass — together with the Pilkey shoulder-fillet stress-concentration penalty into a single normalised number anchored at unity on a reference baseline geometry. To the author's knowledge, no prior peer-reviewed study has introduced a comparable scalar design-selection criterion for AFV torsion bars.

BIBLIOGRAPHY

Benasciutti, D., & Dirlik, T. (2021). Dirlik and Tovo-Benasciutti spectral methods in vibration fatigue: A review with a historical perspective. Metals, 11(9), 1333. https://doi.org/10.3390/met11091333

Benasciutti, D., & Tovo, R. (2018). Frequency-based analysis of random fatigue loads: Models, hypotheses, reality. Materialwissenschaft und Werkstofftechnik, 49(3), 345–367. https://doi.org/10.1002/mawe.201700190

Braun, M., Müller, A. M., Milaković, A.-S., Fricke, W., & Ehlers, S. (2020). Requirements for stress gradient–based fatigue assessment of notched structures according to theory of critical distance. Fatigue & Fracture of Engineering Materials & Structures, 43(7), 1541–1554. https://doi.org/10.1111/ffe.13232

Brnic, J., Brcic, M., Krscanski, S., Lanc, D., Niu, J., & Wang, P. (2018). Steel 51CrV4 under high temperatures, short-time creep and high cycle fatigue. Journal of Constructional Steel Research, 147, 468–476. https://doi.org/10.1016/j.jcsr.2018.05.008

Čerškus, A., Lenkutis, T., Šešok, N., Dzedzickis, A., Viržonis, D., & Bučinskas, V. (2021). Identification of road profile parameters from vehicle suspension dynamics for control of damping. Symmetry, 13(7), 1149. https://doi.org/10.3390/sym13071149

Gagneza, A., & Chandramohan, S. (2019). Estimation of road loads and vibration transmissibility of torsion bar suspension system in a tracked vehicle. Journal of The Institution of Engineers (India): 100(5), 747–761. https://doi.org/10.1007/s40032-018-0460-8

Gomes, V. M. G., Dantas, R., Correia, J. A. F. O., & de Jesus, A. M. P. (2024b). Fatigue crack propagation of 51CrV4 steels for leaf spring suspensions of railway freight wagons. Materials, 17(8), 1831. https://doi.org/10.3390/ma17081831

Gomes, V. M. G., Souto, C. D. S., Correia, J. A. F. O., & de Jesus, A. M. P. (2024a). Monotonic and fatigue behaviour of the 51CrV4 steel with application in leaf springs of railway rolling stock. Metals, 14(3), 266. https://doi.org/10.3390/met14030266

ISO. (2016). ISO 8608:2016 — Mechanical vibration. Road surface profiles. Reporting of measured data. International Organization for Standardization.

James, M. N., Hattingh, D. G., & Matthews, L. (2022). Embrittlement failure of 51CrV4 leaf springs. Engineering Failure Analysis, 139, 106517. https://doi.org/10.1016/j.engfailanal.2022.106517

Jaramillo, H. E., Alba de Sánchez, N., & Avila, J. A. (2019). Effect of the shot peening process on the fatigue strength of SAE 5160 steel. Proceedings of the Institution of Mechanical Engineers, Part C: Journal of Mechanical Engineering Science, 233(8), 2895–2903. https://doi.org/10.1177/0954406218816349

Jeong, S. I., Kim, J. W., Lee, T. K., et al. (2024). Reliability evaluation for shot-peening conditions affecting durability life of automotive suspension coil springs. Engineering Failure Analysis, 161, 108253. https://doi.org/10.1016/j.engfailanal.2024.108253

Khan, A. M., Khalil, M. S., & Azad, M. M. (2025). Estimation of vibration-induced fatigue damage in a tracked vehicle suspension arm at critical locations under real-time random excitations. Machines, 13(4), 257. https://doi.org/10.3390/machines13040257 (Preprint)

Lenkutis, T., Čerškus, A., Šešok, N., Dzedzickis, A., & Bučinskas, V. (2021). Road surface profile synthesis: Assessment of suitability for simulation. Symmetry, 13(1), 68. https://doi.org/10.3390/sym13010068

Múčka, P. (2018). Simulated road profiles according to ISO 8608 in vibration analysis. Journal of Testing and Evaluation, 46(1), 405–418. https://doi.org/10.1520/JTE20160265

Mršnik, M., Slavič, J., & Boltežar, M. (2016). Multiaxial vibration fatigue — A theoretical and experimental comparison. Mechanical Systems and Signal Processing, 76–77, 409–423. https://doi.org/10.1016/j.ymssp.2016.02.012

Pedersen, N. L. (2018). Aspects of stress in optimal shaft shoulder fillet. Journal of Strain Analysis for Engineering Design, 53(5), 285–294. https://doi.org/10.1177/0309324718763514

Saklakoglu, N., Saklakoglu, I. E., Tanrikulu, B., & Yıldız, A. (2021). Effects of shot peening and artificial surface defects on fatigue properties of 50CrV4 steel. International Journal of Advanced Manufacturing Technology, 112(9–10), 2961–2970. https://doi.org/10.1007/s00170-020-06532-y

Singh, A. P., Vidya, S., Suresh, P., Kumar, A., & Srikanth, K. V. N. S. (2022). Comparative stress analysis of round shaft with shoulder fillet using finite element and analytical method. Materials Today: Proceedings, 62(6), 3686–3690. https://doi.org/10.1016/j.matpr.2022.02.168

Tao, J., Deng, Z., Cao, X., Hu, G., & Wang, P. (2024). Modeling and dynamic characteristics of tracked vehicle equipped with symmetrical suspensions based on multi-body dynamics and discrete element coupling method. Applied Sciences, 14(22), 10618. https://doi.org/10.3390/app142210618

Wang, X., Dong, S., Zhang, C., & Jiang, B. (2022). Analysis of torsion bar failure occurring during the pre-strained manufacturing for heavy off-road tracked vehicles. Engineering Failure Analysis, 133, 105956. https://doi.org/10.1016/j.engfailanal.2021.105956

OPTIMIZACIJA GEOMETRIJE TORZIONIH STABILIZATORA OKLOPNIH VOZILA KLASE 30–50 TONA U UVJETIMA VIBRACIJSKOG ZAMORA NA NERAVNIM TERENIMA

Emre Aydin

Agencija za odbrambenu industriju
Ankara, Republika Turska
E-mail: emre.aydin@ssb.gov.tr

Primljeno: 15.01.2025. Prihvaćeno: 11.04.2025.

Originalni naučni članak

DOI: https://doi.org/10.65932/military-studies-2025-1-1
UDK: 623.437.4:621.86.068-034

Sažetak: Torzioni stabilizatori (torzione šipke) i dalje predstavljaju dominantan element primarnog ovjesa kod gusjeničarskih oklopnih platformi klase 30–50 tona — CV90, Puma, K21, Namer, K9 — jer pružaju najvišu specifičnu akumulaciju energije deformacije po jedinici mase od svih izvodljivih jednokomponentnih opruga unutar geometrijskih ograničenja oklopljenog trupa. Njihov dinamički vijek trajanja na kros-kantri terenu usko je vezan za dvije projektne varijable čiji su pojedinačni efekti dobro proučeni, ali čiji zajednički optimum u otvorenoj literaturi nije dovoljno mapiran: odnos radijusa zaobljenja prelaza r_f/d i odnos prečnika aktivne i ramene zone D/d. Ovaj rad razvija spregnuti spektralno-zamorni okvir koji kombinuje Pilkey-jev model koncentracije naprezanja na rameno-zaobljenom prelazu, narrow-band Miner integraciju oštećenja sa Tovo–Benasciutti korekcijom, i ISO 8608 spektralne gustoće pomaka za terene klasa D–F, te predlaže novi bezdimenzionalni Indeks geometrijske zamorne efikasnosti (GFEI) koji spreže kaznu koncentracije naprezanja, geometriju zaobljenja, vitkost aktivne dužine i masu šipke u jedan jedinstven projektni kriterij. Okvir je primijenjen na deset parametarskih scenarija koji pokrivaju raspon borbene mase 33–50 tona i validiran je prema deset sintetičkih S–N tačaka generisanih iz Basquinovih parametara pet SCOPUS-indeksiranih studija (Brnic et al., 2018; Gomes et al., 2024a; Saklakoglu et al., 2021; Jaramillo et al., 2019; Wang et al., 2022), uz Pearsonov koeficijent korelacije r = 0.580, RMSE = 0.73 dekada u log N i regresijski nagib 1.05. Rezultati pokazuju da povećanje r_f/d sa uobičajenih 0.05 na optimum od 0.12–0.16 produžava vijek trajanja na kros-kantri terenu za više od tri reda veličine u neograničenoj Basquinovoj ekstrapolaciji, uz porast mase šipke ispod 3 %. Originalni doprinos rada je GFEI indeks, koji sažima spregnuti geometrijsko-zamorni kompromis u jedan uporedivi skalar i omogućava brzo pretraživanje projektnog prostora prije pune analize metodom konačnih elemenata ili terenskih ispitivanja.
Ključne riječi*: torziona šipka, oklopno vozilo, zamorni vijek, koncentracija naprezanja, ISO 8608, kros-kantri teren, rameno zaobljenje, narrow-band Miner, GFEI, 51CrV4.*